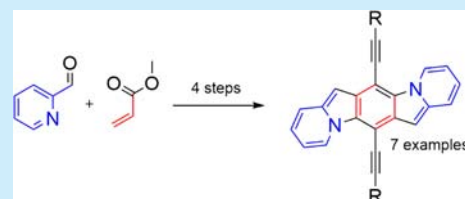


Synthesis and Electrical Properties of Derivatives of 1,4-bis(trialkylsilyl)ethynylbenzo[2,3-*b*:5,6-*b'*]diindolizinesDevin B. Granger,<sup>†</sup> Yaochuan Mei,<sup>‡</sup> Karl J. Thorley,<sup>†</sup> Sean R. Parkin,<sup>†</sup> Oana D. Jurchescu,<sup>‡</sup> and John E. Anthony<sup>\*,†</sup><sup>†</sup>Department of Chemistry, University of Kentucky, Chemistry-Physics Building, 505 Rose Street, Lexington, Kentucky 40506, United States<sup>‡</sup>Department of Physics, Wake Forest University, 1834 Wake Forest Road, Winston-Salem, North Carolina 27109, United States

## Supporting Information

**ABSTRACT:** A new class of nitrogen-containing arene organic semiconductors incorporating fused indolizine units is described. This system, though having a zigzag shape, mimics the electronic properties of its linear analogue pentacene as a result of nitrogen lone pair incorporation into the  $\pi$ -electron system. Solubilizing trialkylsilyl ethynyl groups were employed to target crystal packing motifs appropriate for field-effect transistor devices. The triethylsilyl ethynyl derivative yielded hole mobilities of  $0.1 \text{ cm}^2 \text{ V}^{-1} \text{ s}^{-1}$  and on/off current ratios of  $10^5$ .

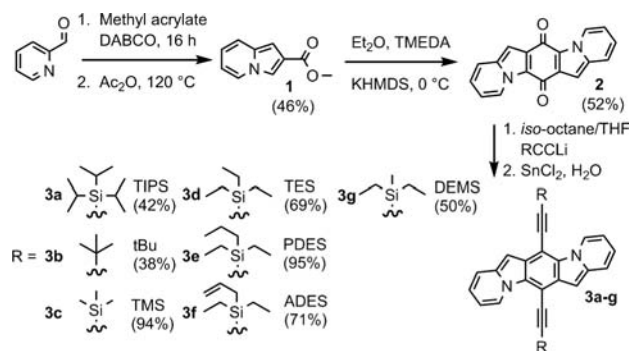


In the past few decades, organic molecules incorporating nontraditional aromatic units, such as azulene,<sup>1</sup> indolizine,<sup>2</sup> and other similar N-heteroarenes,<sup>3</sup> have been investigated for their optoelectronic properties. Recently, a number of organic chromophores for use in photophysical applications have been developed that incorporate the indolizine moiety,<sup>4</sup> a naphthalene analogue with a bridgehead nitrogen. Most of these examples focus primarily of the highly fluorescent nature of the materials and applications related to this property. However, Delcamp and co-workers<sup>4c</sup> demonstrated the potential use of indolizine-based molecules in dye-sensitized solar cells, demonstrating that charge generation and transport are reasonably efficient with these molecules.

The substitution of one or more of the benzene rings in an acene chromophore with another variety of aromatic group greatly affects the optoelectronic properties of the chromophore.<sup>5</sup> This route of functionalizing and tuning acenes opens interesting new avenues in combination with nontraditional aromatics such as indolizine. Here, we report a straightforward route to synthesize N-heteroaromatic compounds that have the indolizine moieties fused into a larger, solubilized chromophore, allowing us to investigate the electronic, optoelectronic, and structural properties in detail.

We incorporated the indolizine moieties into a dibenzoanthracene-like framework through a quinone intermediate, and then ethynylation (see the Supporting Information (SI)) was used to attach solubilizing groups that direct the chromophore's solid-state packing (Scheme 1). The synthesis proceeds through methyl 2-indolizinate (**1**),<sup>6</sup> easily synthesized via the Baylis–Hillman reaction between 2-formylpyridine and methyl acrylate, followed by an intramolecular annulation in acetic anhydride. The subsequent benzo[2,3-*b*:5,6-*b'*]diindolizine (BDI) quinone (**2**) was obtained via an intermolecular nucleophilic annulation reaction. This quinone was then functionalized by ethynylation

## Scheme 1. Synthesis of Benzodiindolizines 3a–g



in isooctane and tetrahydrofuran (THF) solution followed by aromatization with tin(II) chloride in THF to yield ethynyl-substituted BDIs **3a–g**.

It was immediately apparent that the optoelectronic properties of these molecules were significantly different from those of structurally analogous benzo[1,2-*b*:4,5-*b'*]bis[*b*]-benzothiophene.<sup>7</sup> The solution color of the BDI molecules was blue instead of the typical yellow color of anthracene analogues. This result suggests an electronic energy gap similar to that of pentacene, which is confirmed by comparison of the UV–vis spectra as shown in Figure 1. This result is a consequence of the placement of the nitrogen atoms in the aromatic framework of BDI, forcing the nitrogen lone pairs to fully participate in the ring current.

It was expected that the BDI chromophore would not be acid-sensitive because of the incorporation of the nitrogen lone pair

Received: October 4, 2016

Published: November 15, 2016

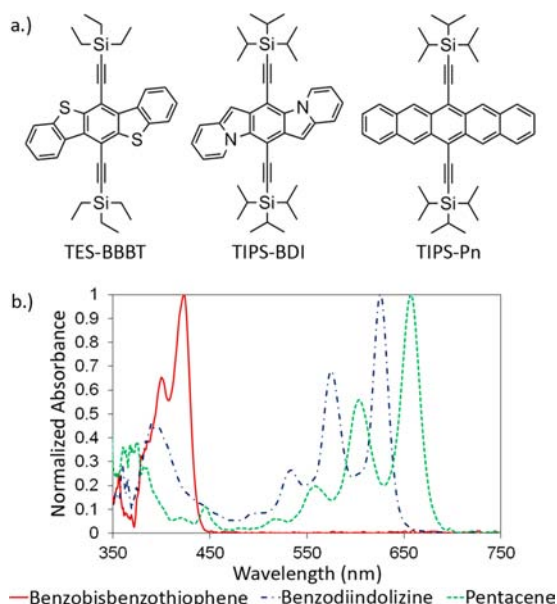


**Figure 1.** (a) Structures of alkylsilyl ethynyl derivatives of benzobis(benzothiophene) (TES-BBBT), benzodiindolizine (TIPS-BDI, **3a**), and pentacene (TIPS-Pn). (b) Comparison of the normalized UV-vis spectra of TES-BBBT (red solid trace), TIPS-BDI (blue dot-dashed trace), and TIPS-Pn (green dashed trace).

into the  $\pi$  electrons of the ring system (as in N1 in imidazoles). Unexpectedly, the BDI molecules are quite sensitive to acidic conditions, requiring acid-free reaction conditions and neutralization of silica when conducting chromatography. Analytical methods such as voltammetry and NMR characterization also require the exclusion of all traces of acid.

It is interesting to note that the acid/base chemistry of BDI is reversible. Protonation of the chromophore appears to occur at the enamine moiety in the five-membered ring (as shown below), and treatment with mild base leads to complete recovery of the BDI chromophore (Figure 2). The site of protonation was identified via  $^1\text{H}$  NMR comparison of TIPS-BDI (**3a**) in carbon disulfide and deuterated chloroform, which is known to contain residual acid.

In these benzodiindolizine molecules, red fluorescence is readily apparent. Fluorescence quantum yields were measured according to literature methods<sup>8</sup> to determine relative values compared to rubrene (see the SI). From this relative measurement, a fluorescence quantum yield of 32% was measured for

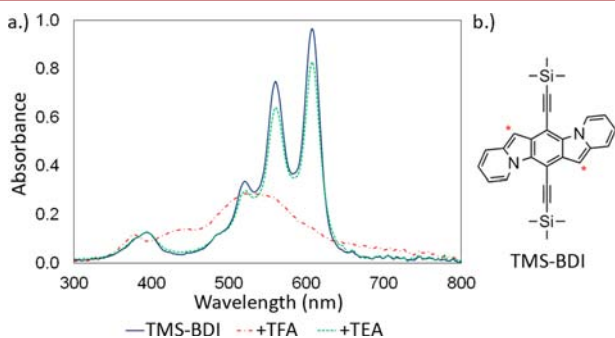


**Figure 2.** (a) UV-vis absorption spectra of a TMS-BDI (**3c**) solution in toluene (blue solid trace), with trifluoroacetic acid (red dot-dashed trace), and then with triethylamine (green dashed trace). (b) Structure of **3c** with basic carbons indicated with red asterisks.

TIPS-BDI using two separate wavelengths (509 and 545 nm). This is substantially higher than those of 6,13-bis-(trialkylsilyl ethynyl)pentacene derivatives, which are less than 10%.<sup>8,9</sup>

Because of the nontraditional aromatic periphery, we were interested to determine the modes of decomposition for these compounds, specifically their reactivity toward dienophiles. The rapid Diels–Alder reaction between pentacenes and fullerenes, for example, has hampered their incorporation into modern organic bulk-heterojunction photovoltaics.<sup>10a</sup> The stability of TIPS-BDI (**3a**) toward light and fullerenes was measured and monitored by UV-vis spectroscopy (see the SI). To measure the light stability, a dilute solution in oxygen-free toluene was irradiated with a 150 W white light source at 50% power. The half-life of the BDI chromophore was on the order of 5 min under these conditions. The reactivity toward fullerenes was also measured in toluene at UV-vis concentrations of a mixture of **3a** and PC<sub>60</sub>BM. Unlike the reactivity of pentacenes with fullerenes,<sup>10</sup> which occurs essentially instantly, no Diels–Alder reaction between TIPS-BDI and PC<sub>60</sub>BM was observed after 3 days in solution.

CV analysis suggested that the oxidation of these BDIs is irreversible, although differential pulse voltammetry (DPV) analysis showed the oxidation to be quasi-reversible (Figure 3).

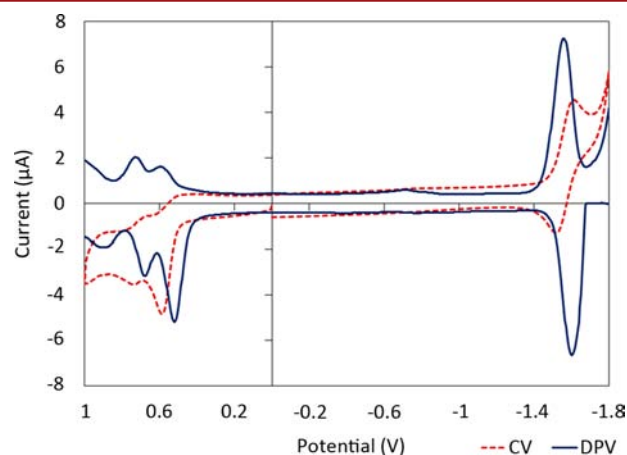


**Figure 3.** Cyclic voltammogram (red trace) and differential pulse voltammogram (blue trace) of TIPS-BDI (**3a**) with 0.1 M Bu<sub>4</sub>NPF<sub>6</sub> in THF.

The discrepancy between these measurements with respect to reversibility stems from differences between the methods, as CV is a continuous-sweep method while DPV is a stepwise (pulsed) measurement, which is less sensitive to sluggish charge transfer kinetics. The first oxidation potential of TIPS-BDI overlaps with the ferrocene/ferrocenium (Fc/Fc<sup>+</sup>) redox pair, placing the BDI highest occupied molecular orbital (HOMO) at approximately −4.83 eV.<sup>11</sup> In contrast to oxidation, the reduction of BDI is reversible.<sup>12</sup> The reduction pair from DPV was used to calculate the approximate lowest unoccupied molecular orbital (LUMO) energy of −2.63 eV. The electrochemically measured frontier molecular orbital (FMO) energy gap is 2.20 eV, which compares well to the optical gap of ~2 eV.

As we have demonstrated with various pentacene derivatives,<sup>13</sup> the solid-state ordering of these BDIs can be influenced by tuning the size and volume of the trialkylsilyl groups employed for solubility. We targeted a 2D “brickwork” arrangement in relation to the central BDI chromophore because of the demonstrated

suitability for field-effect transistors (FETs) when trialkylsilylthynyl-substituted chromophores are used.<sup>14</sup> The trialkylsilyl groups tend to interact with the substrate of the device, and the 2D  $\pi$  stacking is directed along the gap between the source and drain electrodes.<sup>15</sup> We first prepared the triisopropylsilyl (TIPS) derivative to target the 2D “brickwork” motif for the BDI framework. Because of the slightly shorter chromophore, the TIPS-BDI derivative packs in a 1D slip-stack motif (Figure 4a)

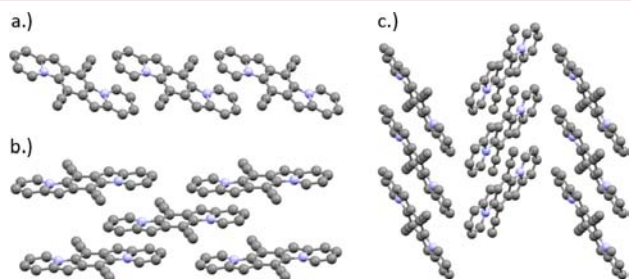


**Figure 4.** Crystal packing diagrams of (a) the TIPS-BDI (3a) 1D slipped-stack motif, (b) the TES-BDI (3d) 2D “brickwork” packing motif, and (c) the DEMS-BDI (3g) 1D “herringbone” packing motif. Alkylsilyl groups have been omitted for clarity.

rather than the target 2D stacking motif. The crystal packing of BDIs functionalized with two smaller solubilizing groups, trimethylsilyl and *tert*-butyl, also yielded 1D slip-stack arrangements similar to that of TIPS-BDI with an added 90° rotation of the central chromophore with respect to adjacent 1D  $\pi$  stacks.

The intended 2D “brickwork” motif was finally realized with triethylsilyl substituents (Figure 4b). Crystals of this material appeared markedly different from other derivatives, growing as plates rather than needles. To gauge the suitability of the BDI derivatives for use in FET devices, we calculated charge transfer integrals (B3LYP/6-31G(d)) based on the crystal structures with Gaussian 09<sup>16</sup> using the method employed by Valeev.<sup>17</sup> The transfer integrals calculated via DFT for HOMO coupling between the two nearest  $\pi$ -stacking neighbors (19 and 31 meV) were comparable to values found for TIPS-pentacene.<sup>18</sup> The transfer integrals for the LUMO coupling of TES-BDI were significantly higher (34 and 49 meV) for these azaacene-like systems,<sup>11,19</sup> but the poor LUMO level alignment for electron injection with the contacts employed in our transistor studies<sup>20</sup> did not allow us to observe n-type behavior.

Subtle changes to the size of the alkylsilyl group reduced the transfer integrals compared with the TES-BDI values. Slightly increasing the size of the substituent proved ineffective: both allyldiethylsilyl (ADES) and *n*-propyldiethylsilyl (PDES) groups yielded similar 2D packing but produced an increase in long-axis slip, reducing the HOMO couplings to 13 and 20 meV for ADES and 4 and 16 meV for PDES. Reducing the size of the alkylsilyl groups proved more interesting: switching from TES to diethylmethylsilyl (DEMS) groups disrupted the 2D  $\pi$ -stacked arrangement and led to a more rubrene-like packing motif (Figure 4c). This change in solid-state packing was accompanied by a change in crystal geometry, yielding crystals of DEMS-BDI as 3D blocks. The calculated transfer integrals for this derivative were 45 meV within the 1D stack and 3 meV for the edge-to-face interaction.

To assess the charge transport in these new chromophores, films of TES-BDI (3d) were deposited by spin-coating from a dilute solution in chlorobenzene/tetralin onto prepatterned

source and drain electrodes that had been treated with pentafluorobenzenethiol (PFBT) to improve the film quality.<sup>22</sup>

The FET device architecture consisted of the BDI molecule film on top of bottom-contact PFBT-treated gold electrodes with Cytop dielectric as the top-gate electrode, following the procedure described elsewhere.<sup>23</sup> These devices showed a maximum hole mobility ( $\mu_h$ ) of 0.1 cm<sup>2</sup> V<sup>-1</sup> s<sup>-1</sup> with on/off current ratios of 10<sup>5</sup> for TES-BDI (Figure 5). Devices fabricated

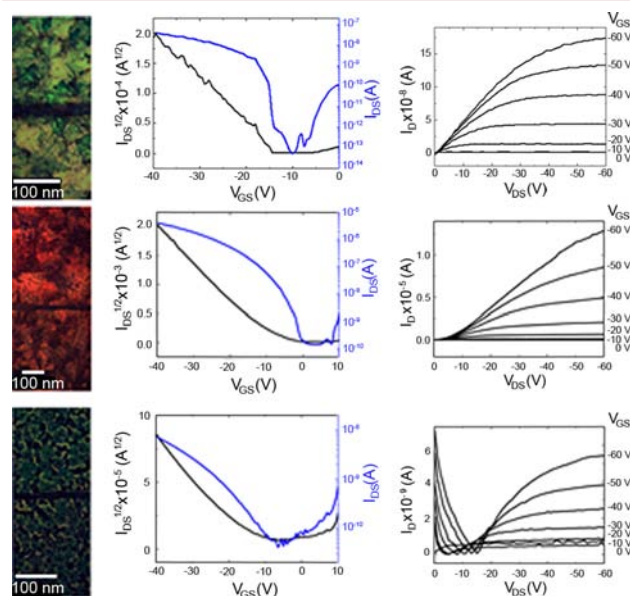


**Figure 5.** Device characteristics of (top) TES-BDI (3d) spin-cast from 10:1 chlorobenzene/tetralin, (middle) PDES-BDI (3e) spin-cast from 8:1 chlorobenzene/tetralin, and (bottom) DEMS-BDI (3g) spin-cast from 1:1 methylene chloride/chlorobenzene. At the left are device film optical images. The middle traces are drain current vs gate voltage characteristics. At the right are output characteristics at various gate voltages.

from PDES-BDI solutions exhibited hole mobilities reaching 0.08 cm<sup>2</sup> V<sup>-1</sup> s<sup>-1</sup>, also with on/off current ratios of 10<sup>5</sup>. We measured over 30 devices from each material and obtained average mobility values of  $0.075 \pm 0.023$  cm<sup>2</sup> V<sup>-1</sup> s<sup>-1</sup> for the TES-BDI derivative and  $0.063 \pm 0.015$  cm<sup>2</sup> V<sup>-1</sup> s<sup>-1</sup> for PDES-BDI. The device performance for these materials is limited because of their poor film-forming properties, likely stemming from their relatively low solubility. Small grains with high boundary area reduce the charge transport efficiency between the source and drain electrodes by increasing the resistance to current flow.<sup>24</sup> This film-forming issue is exacerbated for devices fabricated using DEMS-BDI as the active material because it tends to form films with highly segregated domains, leading to incomplete bridging of the gap between the source and drain electrodes.

The solubility limitations have proved difficult to address for this class of molecules. All of the high-boiling solvents we investigated demonstrated similarly poor solubility and thus would lead to similar film properties. Increasing the size of solubilizing groups in order to alleviate the issue was ineffective, as this resulted in loss of the necessary 2D  $\pi$  stacking in the solid state. We can, however, use the structure–electronic properties relationship of BDI as a guide in the design of new organic chromophores that are less hindered by solubility and subsequent film deposition limitations. We are also exploring the use of additional substituents on the core chromophore to



enhance the transport and impressive fluorescence properties of these compounds as potential light-emitting transistor materials.<sup>21</sup>

## ■ ASSOCIATED CONTENT

### Supporting Information

The Supporting Information is available free of charge on the ACS Publications website at DOI: 10.1021/acs.orglett.6b02991.

Experimental details (PDF)

Crystallographic data for 3c (CIF)

Crystallographic data for 3f (CIF)

Crystallographic data for 3b (CIF)

Crystallographic data for 3g (CIF)

Crystallographic data for 3a (CIF)

Crystallographic data for 3e (CIF)

Crystallographic data for 3d (CIF)

## ■ AUTHOR INFORMATION

### Corresponding Author

\*E-mail: anthony@uky.edu.

### ORCID

John E. Anthony: 0000-0002-8972-1888

### Notes

The authors declare no competing financial interest.

## ■ ACKNOWLEDGMENTS

J.E.A. and D.B.G. thank the Office of Naval Research (N00014-12-1-1007) for support of the synthesis and characterization of new organic semiconductors. The device work was supported by the National Science Foundation under Grant ECCS 1254757.

## ■ REFERENCES

- (1) (a) Kurotobi, K.; Kim, K. S.; Noh, S. B.; Kim, D.; Osuka, A. *Angew. Chem.* **2006**, *118*, 4048. (b) Zhang, X. H.; Li, C.; Wang, W. B.; Cheng, X. X.; Wang, X. S.; Zhang, B. W. *J. Mater. Chem.* **2007**, *17*, 642. (c) Muranaka, A.; Yonehara, M.; Uchiyama, M. *J. Am. Chem. Soc.* **2010**, *132*, 7844.
- (2) Uchida, T.; Matsumoto, K. *Synthesis* **1976**, 1976, 209.
- (3) (a) Kajigaeshi, S.; Mori, S.; Fujisaki, S.; Kanemasa, S. *Bull. Chem. Soc. Jpn.* **1985**, *58*, 3547. (b) Tominaga, Y.; Shiroshta, Y.; Kurokawa, T.; Gotou, H.; Matsuda, Y.; Hosomi, A. *J. Heterocycl. Chem.* **1989**, *26*, 477. (c) Bridge, A. W.; Fenton, G.; Halley, F.; Hursthouse, M. B.; Lehmann, C. W.; Lythgoe, D. J. *J. Chem. Soc., Perkin Trans. 1* **1993**, 2761. (d) Virieux, D.; Guillouzie, A. F.; Cristau, H. J. *Tetrahedron* **2006**, *62*, 3710. (e) Huang, H.; Ji, X.; Tang, X.; Zhang, M.; Li, X.; Jiang, H. *Org. Lett.* **2013**, *15*, 6254.
- (4) (a) Coffinier, D.; El Kaim, L. E.; Grimaud, L. *Synlett* **2010**, 2010, 2474. (b) Wan, J.; Zheng, C.-J.; Fung, X.-K.; Liu, X.-K.; Lee, C.-S.; Zhang, X.-H. *J. Mater. Chem.* **2012**, *22*, 4502. (c) Kim, E.; Lee, Y.; Lee, S.; Park, S. B. *Acc. Chem. Res.* **2015**, *48*, 538. (d) Zhang, Y.; Garcia-Amorós, J.; Captain, B.; Raymo, F. M. *J. Mater. Chem. C* **2016**, *4*, 2744. (e) Huckaba, A. J.; Giordano, F.; McNamara, L. E.; Dreux, K. M.; Hammer, N. I.; Tschumper, G. S.; Zakeeruddin, S. M.; Grätzel, M.; Nazeeruddin, M. K.; Delcamp, J. H. *Adv. Energy Mater.* **2015**, *5*, 1401629.
- (5) (a) Dickey, K. C.; Anthony, J. E.; Loo, Y. L. *Adv. Mater.* **2006**, *18*, 1721. (b) Tsuji, H.; Shoyama, K.; Nakamura, E. *Chem. Lett.* **2012**, *41*, 957. (c) Mori, T.; Nishimura, T.; Yamamoto, T.; Doi, I.; Miyazaki, E.; Osaka, I.; Takimiya, K. *J. Am. Chem. Soc.* **2013**, *135*, 13900. (d) Zhang, J.; Smith, Z. C.; Thomas, S. W., III. *J. Org. Chem.* **2014**, *79*, 10081.
- (6) Bode, M. L.; Kaye, P. T. *J. Chem. Soc., Perkin Trans. 1* **1990**, 2612.

(7) Grimminger, M. L. Periodic Trends in Structure Function Relationship of Organic Heteroacenes. Ph.D. Dissertation, University of Kentucky, Lexington, KY, 2011.

(8) Wolak, M. A.; Melinger, J. S.; Lane, P. A.; Palilis, L. C.; Landis, C. A.; Delcamp, J.; Anthony, J. E.; Kafafi, Z. H. *J. Phys. Chem. B* **2006**, *110*, 7928.

(9) Wolak, M. A.; Jang, B. B.; Palilis, L. C.; Kafafi, Z. H. *J. Phys. Chem. B* **2004**, *108*, 5492.

(10) (a) Miller, G. P.; Briggs, J.; Mack, J.; Lord, P. A.; Olmstead, M. M.; Balch, A. L. *Org. Lett.* **2003**, *5*, 4199. (b) Sarova, G. H.; Berberan-Santos, M. N. *Chem. Phys. Lett.* **2004**, *397*, 402. (c) Cao, Y.; Liang, Y.; Zhang, L.; Osuna, S.; Hoyt, A. L. M.; Briseno, A. L.; Houk, K. N. *J. Am. Chem. Soc.* **2014**, *136*, 10743. (d) Zhang, L.; Cao, Y.; Colella, N. S.; Liang, Y.; Brédas, J. L.; Houk, K. N.; Briseno, A. L. *Acc. Chem. Res.* **2015**, *48*, 500.

(11) Pommerehne, J.; Vestweber, H.; Guss, W.; Mahrt, R. F.; Bässler, H.; Porsch, M.; Daub, J. *Adv. Mater.* **1995**, *7*, 551.

(12) (a) Ahmed, E.; Earmme, T.; Ren, G.; Jenekhe, S. A. *Chem. Mater.* **2010**, *22*, 5786. (b) Bunz, U. H. F.; Engelhart, J. U.; Lindner, B. D.; Schaffroth, M. *Angew. Chem., Int. Ed.* **2013**, *52*, 3810. (c) An, C.; Guo, X.; Baumgarten, M. *Cryst. Growth Des.* **2015**, *15*, 5240.

(13) (a) Anthony, J. E.; Eaton, D. L.; Parkin, S. R. *Org. Lett.* **2002**, *4*, 15. (b) Chen, J.; Subramanian, S.; Parkin, S. R.; Siegler, M.; Gallup, K.; Haughn, C.; Martin, D. C.; Anthony, J. E. *J. Mater. Chem.* **2008**, *18*, 1961. (c) Shu, Y.; Lim, Y. F.; Li, Z.; Purushothaman, B.; Hallani, R.; Kim, J. E.; Parkin, S. R.; Malliaras, G. G.; Anthony, J. E. *Chem. Sci.* **2011**, *2*, 363.

(14) Sheraw, C. D.; Jackson, T. N.; Eaton, D. L.; Anthony, J. E. *Adv. Mater.* **2003**, *15*, 2009.

(15) Chen, J.; Martin, D. C.; Anthony, J. E. *J. Mater. Res.* **2007**, *22*, 1701.

(16) Frisch, M. J.; Trucks, G. W.; Schlegel, H. B.; Scuseria, G. E.; Robb, M. A.; Cheeseman, J. R.; Scalmani, G.; Barone, V.; Mennucci, B.; Petersson, G. A.; Nakatsuji, H.; Caricato, M.; Li, X.; Hratchian, H. P.; Izmaylov, A. F.; Bloino, J.; Zheng, G.; Sonnenberg, J. L.; Hada, M.; Ehara, M.; Toyota, K.; Fukuda, R.; Hasegawa, J.; Ishida, M.; Nakajima, T.; Honda, Y.; Kitao, O.; Nakai, H.; Vreven, T.; Montgomery, J. A., Jr.; Peralta, J. E.; Ogliaro, F.; Bearpark, M.; Heyd, J. J.; Brothers, E.; Kudin, K. N.; Staroverov, V. N.; Kobayashi, R.; Normand, J.; Raghavachari, K.; Rendell, A.; Burant, J. C.; Iyengar, S. S.; Tomasi, J.; Cossi, M.; Rega, N.; Millam, J. M.; Klene, M.; Knox, J. E.; Cross, J. B.; Bakken, V.; Adamo, C.; Jaramillo, J.; Gomperts, R.; Stratmann, R. E.; Yazyev, O.; Austin, A. J.; Cammi, R.; Pomelli, C.; Ochterski, J. W.; Martin, R. L.; Morokuma, K.; Zakrzewski, V. G.; Voth, G. A.; Salvador, P.; Dannenberg, J. J.; Dapprich, S.; Daniels, A. D.; Farkas, Ö.; Foresman, J. B.; Ortiz, J. V.; Cioslowski, J.; Fox, D. J. *Gaussian 09*, revision A.02; Gaussian, Inc.: Wallingford, CT, 2009.

(17) Valeev, E. F.; Coropceanu, V.; da Silva Filho, D. A.; Salman, S.; Brédas, J. L. *J. Am. Chem. Soc.* **2006**, *128*, 9882.

(18) Troisi, A.; Orlandi, G.; Anthony, J. E. *Chem. Mater.* **2005**, *17*, 5024.

(19) (a) Liu, Y. Y.; Song, C. L.; Zeng, W. J.; Zhou, K. G.; Shi, Z. F.; Ma, C. B.; Yang, F.; Zhang, H. L.; Gong, X. *J. Am. Chem. Soc.* **2010**, *132*, 16349. (b) Bunz, U. H. F. *Acc. Chem. Res.* **2015**, *48*, 1676. (c) Schwaben, J.; Münster, N.; Klues, M.; Breuer, T.; Hofmann, P.; Harms, K.; Witte, G.; Koert, U. *Chem. - Eur. J.* **2015**, *21*, 13758. (d) Jahng, Y.; Karim, M. *Tetrahedron* **2016**, *72*, 199.

(20) (a) Jones, B. A.; Facchetti, A.; Wasielewski, M. R.; Marks, T. J. *J. Am. Chem. Soc.* **2007**, *129*, 15259. (b) Cheng, X.; Noh, Y. Y.; Wang, J.; Tello, M.; Frisch, J.; Blum, R. P.; Vollmer, A.; Rabe, J. P.; Koch, N.; Sirringhaus, H. *Adv. Funct. Mater.* **2009**, *19*, 2407.

(21) (a) Zhang, C.; Chen, P.; Hu, W. *Small* **2016**, *12*, 1252. (b) Liu, Z.; Zhang, G.; Zhang, D. *Chem. - Eur. J.* **2016**, *22*, 462.

(22) Ward, J. M.; Li, R.; Obaid, A.; Payne, M. M.; Smilgies, D. M.; Anthony, J. E.; Amassian, A.; Jurchescu, O. D. *Adv. Funct. Mater.* **2014**, *24*, 5052.

(23) Hallani, R. K.; Thorley, K. J.; Mei, Y.; Parkin, S. R.; Jurchescu, O. D.; Anthony, J. E. *Adv. Funct. Mater.* **2016**, *26*, 2341.

(24) Teague, L. C.; Hamadani, B. H.; Jurchescu, O. D.; Subramanian, S.; Anthony, J. E.; Jackson, T. N.; Richter, C. A.; Gundlach, D. J.; Kushmerick, J. G. *Adv. Mater.* **2008**, *20*, 4513.